AUTHOR(S): RUTTKAY-NEDECKY, B., SKALICKOVA, S., KEPINSKA, M., CIHALOVA, K., DOCEKALOVA, M., STANKOVA, M., UHLIROVA, D., FERNANDEZ, C., SOCHOR, J., MILNEROWICZ, H., BEKLOVA, M. and KIZEK, R.

TITLE: Development of new silver nanoparticles suitable for materials with antimicrobial properties.

YEAR: 2019

Publisher citation: RUTTKAY-NEDECKY, B., SKALICKOVA, S., KEPINSKA, M., CIHALOVA, K., DOCEKALOVA, M., STANKOVA, M., UHLIROVA, D., FERNANDEZ, C., SOCHOR, J., MILNEROWICZ, H., BEKLOVA, M. and KIZEK, R. 2019. Development of new silver nanoparticles suitable for materials with antimicrobial properties. Journal of nanoscience and nanotechnology [online], 19(5), pages 2762-2769. Available from: https://doi.org/10.1166/jnn.2019.15867

OpenAIR citation: RUTTKAY-NEDECKY, B., SKALICKOVA, S., KEPINSKA, M., CIHALOVA, K., DOCEKALOVA, M., STANKOVA, M., UHLIROVA, D., FERNANDEZ, C., SOCHOR, J., MILNEROWICZ, H., BEKLOVA, M. and KIZEK, R. 2019. Development of new silver nanoparticles suitable for materials with antimicrobial properties. Journal of nanoscience and nanotechnology, 19(5), pages 2762-2769. Held on OpenAIR [online]. Available from: https://openair.rgu.ac.uk

Article

Journal of
Nanoscience and Nanotechnology
Vol. 18, 1–8, 2018
www.aspbs.com/jnn

Development of New Silver Nanoparticles Suitable for Materials with Antimicrobial Properties

Branislav Ruttkay-Nedecky[1], Sylvie Skalickova[1], Marta Kepinska[2], Kristyna Cihalova[1], Michaela Docekalova[1], Martina Stankova[1], Dagmar Uhlirova[1], Carlos Fernandez[3], Jiri Sochor[1], Halina Milnerowicz[2], Miroslava Beklova[4], and Rene Kizek[1, 2, *]

[1] *Central Laboratory, Faculty of Pharmacy, University of Veterinary and Pharmaceutical Sciences Brno, Brno, Czech Republic*
[2] *Wroclaw Medical University, Faculty of Pharmacy, Department of Biomedical and Environmental Analyses, Wroclaw, Poland*
[3] *School of Pharmacy and Life Sciences, Robert Gordon University, Aberdeen, United Kingdom*
[4] *Department of Ecology and Diseases of Game, Fish and Bees, University of Veterinary and Pharmaceutical Sciences Brno, Brno, Czech Republic*

Silver nanoparticles are the most important nanoparticles in connection with the antimicrobial effect. Nowadays, the green synthesis of various types of nanoparticles is rapid, effective and produce less toxic nanoparticles often with specific properties. In our experiment we have developed and described in details various types of silver nanoparticles synthesized chemically or by the green synthesis. Nine different silver nanoparticles were synthesized, three by citrate method at different pHs (8; 9; 10), four using gallic acid at alkaline pHs (10; 11), and two by green synthesis using green tea and coffee extracts, both at pH 9. Characterisation of silver nanoparticles was performed using dynamic light scattering, scanning electron microscopy, and ultraviolet–visible absorption spectroscopy. Silver nanoparticles prepared by green synthesis showed the highest antioxidant activity and also ability for quenching of free radicals. Antibacterial activity of silver nanoparticles was determined on bacterial cultures such as *Staphylococcus aureus* and *Escherichia coli*. Silver nanoparticles synthesized using green tea and coffee extracts showed the highest antibacterial activity for both bacterial strains. Minimal inhibition concentration for both strains was found to be 65 μM at each silver nanoparticle synthesized using green synthesis.

Keywords: Silver Nanoparticles, Antioxidant Activity, Antimicrobial Activity, Green Synthesis.

1. INTRODUCTION

Due to the increasing bacterial resistance to classic antibiotics, the investigations on the antibacterial activity of silver nanoparticles have increased over the last few decades.[1, 2] The antibacterial activity of silver species has been well known since ancient Greece[2–4] and it has been demonstrated that, in low concentrations, silver is non-toxic to human cells.[5] Currently, the investigation of this phenomenon has regained importance due to the increase of bacterial resistance to antibiotics, caused by their overuse.[6]

Antibacterial activity of the silver-containing materials can be used, for example, in medicine to reduce infections in burn treatment and arthroplasty, as well as to prevent bacteria colonization on prostheses, catheters, vascular grafts, dental materials, stainless steel materials, and human skin.[7, 8] Contrary to bactericide effects of ionic silver, the antimicrobial activity of colloid silver nanoparticles is influenced by the dimensions of the particles. The smaller the particles, the greater the antimicrobial effect is, this is due to better penetration of smaller nanoparticles (1–10 nm) into bacterial cells.[9] Silver nanoparticles exhibiting antimicrobial activity have been synthesized by utilizing different methodologies.[2–5, 10] The most common method to synthesize silver nanoparticles is the chemical reduction of a silver salt solution by a reducing agent such as $NaBH_4$, citrate, and ascorbate. The use of a strong reductant e.g., chemical compound such as borohydride, results in the formation of small particles (20–45 nm). On the other hand the use of citrate, a weaker reductant,

*Author to whom correspondence should be addressed.

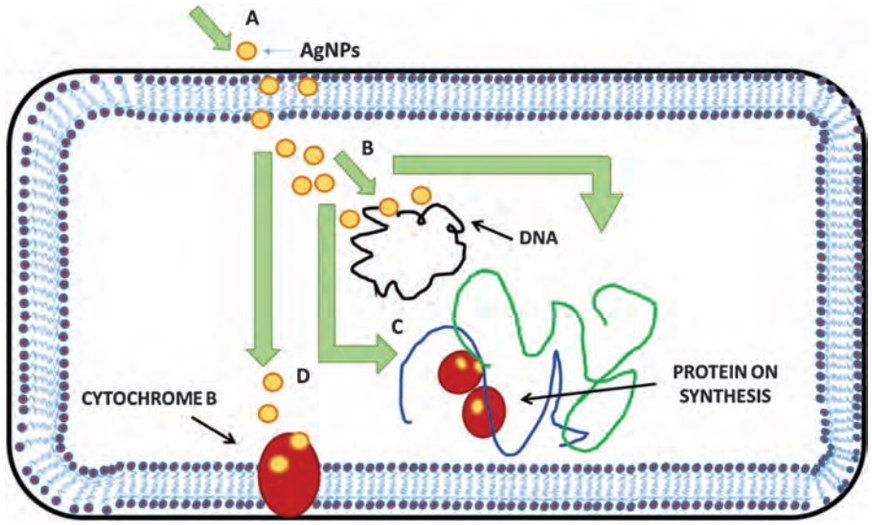

Figure 1. Proposed mechanisms of action of silver nanoparticles AgNPs (or Ag^+ coming from AgNPs) on bacteria. (A) AgNPs penetrate the bacterial cell wall and may bind to the phospholipid bilayer of the cytoplasmic membrane; (B) AgNPs may bind the bacterial DNA with subsequent disrupting of DNA replication; (C) AgNPs may impair the ability of ribosomes to transcribe messenger RNA; (D) AgNPs may bind to the sulfhydryl group of the cytochrome b. Adopted and modified according to Ricco and Assadian.[8]

resulted in a slower reduction rate, with a wide distribution size varying from 20–170 nm.[2]

Inorganic conventional synthesis of nanoparticles using physical methods are used for preparation of antibacterial nanoparticles. This process is demanding for chemicals, instruments and energy. In recent years, the main goal of research has been focused on the development of efficient methods of organic chemistry for synthesis of metallic nanoparticles. Often used approach is the production of metal nanoparticles using organisms such as plants. Nanoparticles produced by plants are stable and the rate of synthesis is faster than in the case of microorganisms which is one of the other possibilities of green synthesis.[11] The green biosynthesis is based on the reduction of metal ions to nanoparticles by biomolecules present in plant extracts. For green biosynthesis is possible to use plant extracts and live plants.[12] Biogenic AgNPs are functionalized with phytochemical coating, rendering them more biologically active as compared with chemically synthesized AgNPs.[13] Eco-friendly plants containing proteins, which act as both reducing and capping agents form a stable and shape-controlled AgNPs. Mechanism of antibacterial effect of AgNPs modified by surfactants polymers is discussed in terms of its interaction with cell membrane against Gram-positive and Gram-negative bacteria.[10] The intensity of antibacterial effect depends on the type of cell membrane.

The actual bactericide mechanism of silver nanoparticles is not well known. Some researchers support the idea that silver species release Ag^+ ions that interact with the thiol groups within the proteins in the bacteria, affecting there application of DNA.[7] It has also been reported that Ag^+ ions either uncouple the respiratory chain from oxidative phosphorylation or collapse the proton-motive force across the cytoplasmic membrane.[3] Silver nanoparticles interactions with bacteria depend on the size and shape of the nanoparticles.[2,5,9] Several studies have been reported to explain the inhibitory effect of silver on bacteria, and it is generally believed that silver ions interact with proteins by reacting either with the thiol groups of methionine or cysteine amino acids of the active site of the enzymes, leading to the inactivation of the proteins. In particular, Feng et al.[14] reported that silver ions affect the DNA replication capability, which in turn induces the inactivation of bacterial proteins (Fig. 1).

In this work, we used different approaches for silver nanoparticles'synthesis. We utilized the classical citrate method, then reduction using gallic acid at alkaline pH, and finally green synthesis using green tea and coffee extracts. The obtained nanoparticles were characterized using dynamic light scattering (DLS), scanning electron microscopy (SEM), and ultraviolet-visible (UV-vis) absorption spectroscopy. An antioxidant approach and antibacterial activity test was conducted to observe differences in antibacterial activity among the various types of silver nanoparticles.

2. EXPERIMENTAL DETAILS

2.1. Chemical

All the chemicals used in this study ($AgNO_3$, $NaBH_4$, gallic acid, trisodium citrate dihydrate, NaOH) were purchased from Sigma-Aldrich (St. Louis, MO, USA) in ACS purity. $NaBH_4$ was purchased from (Merck, Darmstadt, Germany), 25% NH_4OH water solution was purchased from Lach-Ners.r.o. (Neratovice, Czech Republic). Deionized water was prepared using reverse osmosis equipment

Aqual 25 (Brno, Czech Republic). Deionized water was further purified by using a MiliQ Direct QUV apparatus equipped with a UV lamp. The resistance was 18 MΩ. The pH was measured using a pH meter WTW inoLab (Weilheim, Germany).

2.2. Preparation of Silver Nanoparticles

2.2.1. AgNPs-A, B, C

Silver nanoparticles were prepared according to Wan et al.[15] with a minor modification. 500 μL of 0.1 M $AgNO_3$ was mixed with 49 mL of distilled water. Then, 1650 μL of 1% tri-sodium citrate was added dropwise. Subsequently, 10 mL of 10 mM $NaBH_4$ (A) or 10 mL of 5 mM $NaBH_4$ (B) or 10 mL of 20 mM $NaBH_4$ (C) were added and the solution was stirred for 1 hour to change the colour to yellow, indicating the formation of particles. The resulting pH was as follows: for A 9.2, for B 7.7, and for C 9.6.

2.2.2. AgNPs-D, E, F, G

100 mL of 0.001 M $AgNO_3$ was mixed with 10 mL of gallic acid (1 mg/mL) and the solution was stirred for 1 hour to change the colour to yellow. The pH was then adjusted with 1 M NaOH to 11.0 (D) or with NH_4OH (25%) to pH 10 (E) or with 1 M NaOH to pH 10 (F) or with NH_4OH (25%) to pH 11 (G).

2.2.3. AgNPs-H, I

2 g of green tea (H) or coffee (I) was dipped in 100 mL of distilled water. The solution was heated to 80 °C for 20 min (H) or for 5 min (I). The solution was then cooled and filtered. The filtrate obtained was used as a reducing agent. A 1:1 solution of 0.1 M $AgNO_3$ was mixed with the filtrate obtained. The mixed solution was allowed to stir for 24 hours at room temperature.

2.3. Scanning Electron Microscopy

Structure of AgNPs was characterized by SEM. For documentation of the nanoparticles structure a MIRA3 LMU (Tescan, Brno, Czech Republic) was used. This model is equipped with a high brightness Schottky field emitter for low noise imaging at fast scanning rates. The SEM was fitted with In-Beam SE detector. An accelerating voltage of 15 kV and beam currents about 1 nA gives satisfactory results regarding maximum throughput. Magnification for AgNPs 40 kX was used.

2.4. Dynamic Light Scattering

The average particle size and size distribution were determined using dynamic laser light scattering with a Malvern Zetasizer (NANO-ZS, Malvern Instruments Ltd., Worcestershire, U.K.). Nanoparticle distilled water solution of 1.5 mL (1 mg/mL) was put into a optically homogeneous square polystyrene cells and measured at a detector angle of 173°, a wavelength of 633 nm, a refractive index of 0.30, a real refractive index of 1.59, and a temperature 25 °C.

The particle charge (ζ-potential) was measured by the microelectrophoretic method at 25 °C in polycarbonate cuvettes. Each value was obtained as an average of five subsequent runs of the instrument with at least 20 measurements.

2.5. UV-Vis Spectrometry

The optical properties of nanoparticles were studied by spectral analysis. The absorbance spectra of nanoparticles were recorded within the range from 350 to 700 nm using an UV-3100PC UV-VIS spectrophotometer (VWR, Germany).

2.6. Cultivation of *Staphylococcus aureus* and *Escherichia coli*

Staphylococcus aureus and *Escherichia coli* were obtained from the Czech Collection of Microorganisms, Faculty of Science, Masaryk University, Brno, Czech Republic. Strains were stored in the form of a spore suspension in 20% (v/v) glycerol at −20 °C. Prior to use, the strains were thawed and the glycerol was removed by washing with distilled water in this study. The composition of the cultivation medium was described as follows: meat peptone 5 g L^{-1}, NaCl 5 g L^{-1}, bovine extract 1.5 g L^{-1}, yeast extract 1.5 g L^{-1} (HIMEDIA, Mumbai, India), sterilized MilliQ water. The pH value of the cultivation medium was adjusted at 7.4 before sterilization. Sterilization of media was carried out at 121 °C for 30 min in a sterilizer (Tuttnauer 2450EL, Beit Shemesh, Israel). The prepared cultivation media were inoculated with bacterial culture into 25 mL Erlenmeyer flasks. After the inoculation, bacterial cultures were cultivated for 24 h on a shaker at 600 rpm and 37 °C. Bacterial culture cultivated under these conditions was diluted with cultivation medium to OD600 = 0.1 and used in the following experiments.

2.7. Determination of Antibacterial Properties

To determine the antimicrobial effect of silver nanoparticles (AgNPs) the measurement of the inhibition zones was performed. Agar surface in Petri dish was covered with a mixture of 100 mL of 24 h culture of *S. aureus* or *E. coli* in the exponential phase of growth, and 3 mL of LB medium (Luria Bertani medium). Excess volume of the mixture of the Petri dishes was aspirated. Petri dishes were insulated against possible external contamination and placed in a thermostat (Tuttnauer 2450EL, Beit Shemesh, Israel) set at 37 °C for 24 h. After 24 h of incubation, the inhibition zones were measured and photographed in each Petri dish.

To determine the antimicrobial effect of tested AgNPs by the growth curve method the absorbance using the apparatus Tecan Infinite 200 PRO (TECAN, Switzerland) was measured. In the microplate *S. aureus* and *E. coli*

was mixed with various concentrations of AgNPs or alone as a control for the measurements. The concentrations of AgNPs in samples A–G were 0, 1.25, 10, 40 and 160 μM. The concentrations of AgNPs in samples H and I were 0, 0.065, 0.52, 2.1 and 8.3 mM. Total volume of mixture in the Greiner 96 well transparent microplate (Sigma Aldrich, St. Louis, MO, USA) was always 300 μL. The absorbance was measured at wavelength 600 nm for 20 hours every 30 minutes.

2.8. Determination of Quenching of Artificial Radicals

Spectrophotometric measurements of oxidative stress were carried out using an automated chemical analyser BS-200 (Mindray, Shenzhen, China). Reagents and samples were placed on cooled sample holder (4 ± 1 °C) and automatically pipetted directly into plastic cuvettes. Incubation proceeded at 37.0 ± 0.1 °C. Mixture was consequently stirred. The washing steps of pipetting needle with distilled water (18 mΩ) were carried out in the midst of the pipetting. The instrument was operated using the BS-200 software.

2.8.1. N,N-Dimethyl-1,4-Diaminobenzene (DMPD) Method

DMPD radical scavenging activity of AgNPs was performed as follows: The compound *N*,*N*-dimethyl-1,4-diaminobenzene (DMPD) is converted in solution to a relatively stable and coloured radical form ($DMPD^{\cdot+}$) by the action of ferric salt. After addition of a sample containing antioxidants, $DMPD^{\cdot+}$ radicals are scavenged and as a result of this scavenging, the coloured solution is decolourized.[16]

A 160 μL volume of reagent (200 mM DMPD, 0.05 M $FeCl_3$, 0.1 M acetate buffer pH 5.25) was injected into a plastic cuvette with subsequent addition of 4 μL sample. Absorbance was measured at 505 nm. Difference between absorbance at the last (12th) minute and second minute of the assay procedure was used for calculating the antioxidant activity. The percentage of radicals, that were not scavenged, was measured.

2.8.2. Free Radicals (FR) Method

This method is based on the ability of chlorophyllin (the sodium-copper salt of chlorophyll) to accept and donate electrons with a stable change of maximum absorption. This effect is conditioned by an alkaline environment and the addition of a catalyst. A 150 μL volume of reagent was injected into a plastic cuvette with the subsequent addition of a 6 μL sample. The absorbance was measured at 450 nm in the second minute of assay and for the last (12th) minute. The difference between these two values is considered as an outputting value.[17]

2.8.3. Statistic and Results Evaluation

Data were processed using MICROSOFT EXCEL® (USA). Results are expressed as mean ± standard deviation (S.D.) unless noted otherwise (EXCEL®). All the obtained data are stored in the Ladys database.

3. RESULTS AND DISCUSSION

Three different approaches of AgNPs synthesis have been applied. The first approach was the chemical synthesis based on the reduction of Ag^+ ions using $NaBH_4$ at different concentrations (samples A–C). The second approach was the preparation of AgNPs with gallic acid at various pH (samples D–G). The third approach was the preparation of AgNPs using green synthesis. For the green synthesis we used green tea and coffee extracts which are able to reduce Ag^+ ions and induce nanoparticle formation (samples H–I). The obtained solutions are shown in the Figure 2.

3.1. Characterization of AgNPs

The characterization of AgNPs is necessary for their confirmation, determination of their size and stability properties which could play a role in their antibacterial activity. We used size measurement and *Z*-potential characterization of colloidal state of the nanoparticle system as well as scanning electron microscopy (SEM) to obtain detailed AgNPs structure. The summary of obtained results is shown in Figure 3. SEM depicts the spherical shape of AgNPs as well as the formation of clusters. Samples A, F, H and I show enhanced increase in surface charging which could be the result of used reduction agent. Nanoparticle size was determined using dynamic light scattering measurement. From all samples, the size varies in the range of 80–85 nm and it is clearly evident that the dependence of the preparation conditions did not have an effect on the particle size.

Measurement of the zeta potential (or charge density) of samples provides important information for predicting their binding capacity and stability. Generally, a higher zeta potential than 30 or −30 mV indicate good stability of the nanoparticles in the colloidal system. Our synthesized nanoparticles show negative charge and the values of the zeta potential are in the range of -22.5 ± 3.5 mV in all cases A–I. Poor stability of colloidal system could lead to slight nanoparticle agglomeration which was confirmed by SEM.

3.2. The Spectral Analysis of AgNPs

UV-VIS spectroscopy of the prepared samples could provide information about the change of the sample spectra in dependence of the preparation protocol. The synthesized AgNPs in aqueous solution were monitored by recording the absorption spectra at a wavelength range of 250–650 nm (Fig. 4). Nanoparticles made of silver, strongly interact with specific wavelengths of light and show the unique optical properties. The change of the AgNPs spectrum, depends on their aggregation or formation of different AgNPs. Thus, the variety of AgNPs formation could

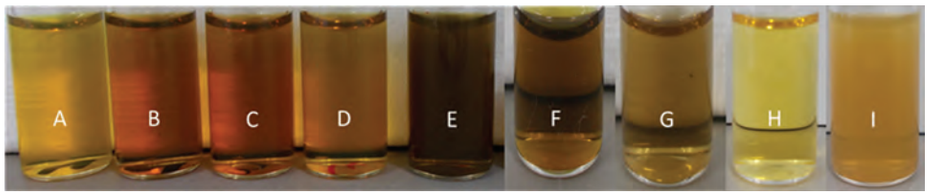

Figure 2. AgNPs formed by two ways of chemical synthesis using different reduction agents (A–C) $NaBH_4$ and (D–G) gallic acid at various pH. Samples H and I are AgNPs produced by the green synthesis using tea and coffee extracts. The preparation protocol for each AgNPs are shown in materials and methods.

be attributed to electrons near each particle surface which become delocalized and are shared amongst neighbouring particles. In the case of samples A–B which were reduced by $NaBH_4$, it was obvious that a similar trend with the absorbance maxima near 400 nm was obtained indicating a good agreement with Deepak et al.[18] Absorbance spectra of samples D–G showed different trends. In the case of sample D, a shift of absorbance maximum to the shorter wavelength 351 nm is obvious while sample F shows a shift of absorbance maximum to the longer wavelength 423 nm. Those values are opposite to what it would be expected for a characteristic AgNPs spectra. Spectrum of sample G shows two absorbance maximum peaks at 300 and 374 nm. A similar trend is visible for sample E, where the absorbance maxima nearly correspond to the sample G. AgNPs formed employing a green synthesis show different absorbance spectra compared to other conventional methods of synthesis. Two characteristic absorbance maximum peaks for sample H at 250 and 400 nm and for sample I at 280 and 508 nm can be observed. This unusual spectrum course of AgNPs could be caused by the incorporation of reducing substances from coffee and tea extracts. It was estimated, that the characteristic spectra of green synthesized AgNPs vary in their dependence course of used plant extract.[19]

3.3. Determination of the Quenching Activity

To determine the quenching activity of the tested AgNPs, we choose an appropriate assay employing DMPD method. This assay is based on the reduction of buffered coloured solution of DMPD in acetate buffer and ferric chloride. The procedure involves measurement of decrease in absorbance of DMPD in the presence of scavengers at its absorption maximum of 505 nm. The activity is expressed as percentage reduction of DMPD.[20] Graph (Fig. 4(D)) shows the ability of AgNPs quenching DMPD radicals expressed as percentage of radicals that were not scavenged. Samples A–E show similar quenching activity (75%) independently on the preparation process while F, G (88, 93%) evinced weak ability for quenching of DMPD

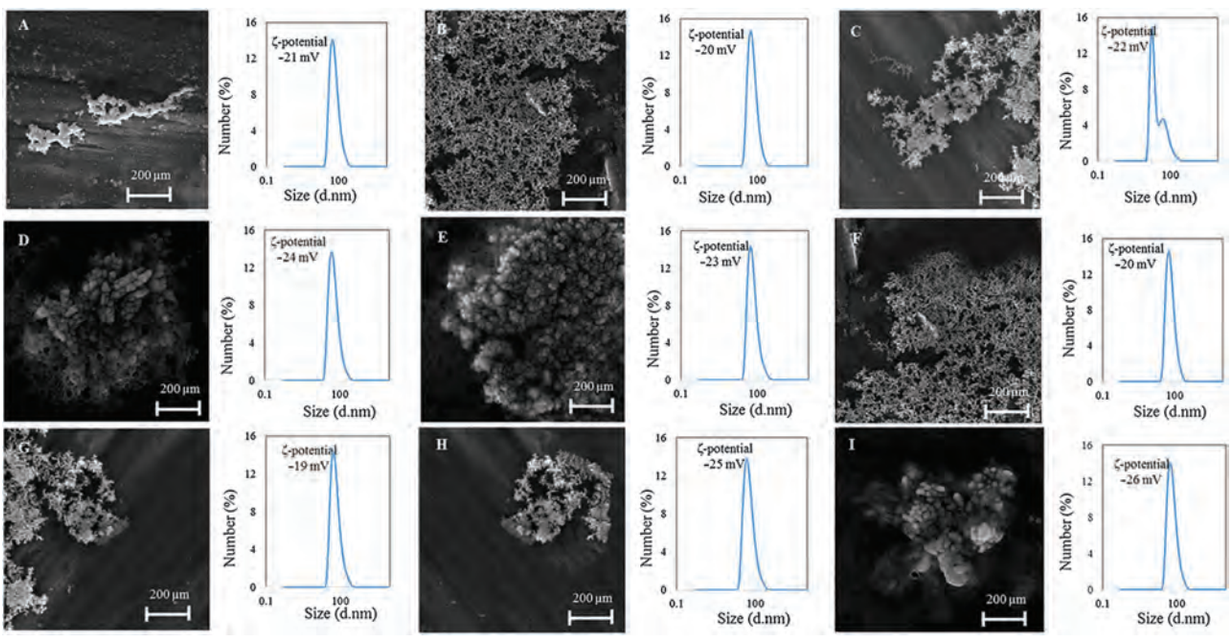

Figure 3. Photographs of prepared AgNPs (A–I) obtained by SEM and their sizes determined using dynamic light scattering. Further details are described in material and methods.

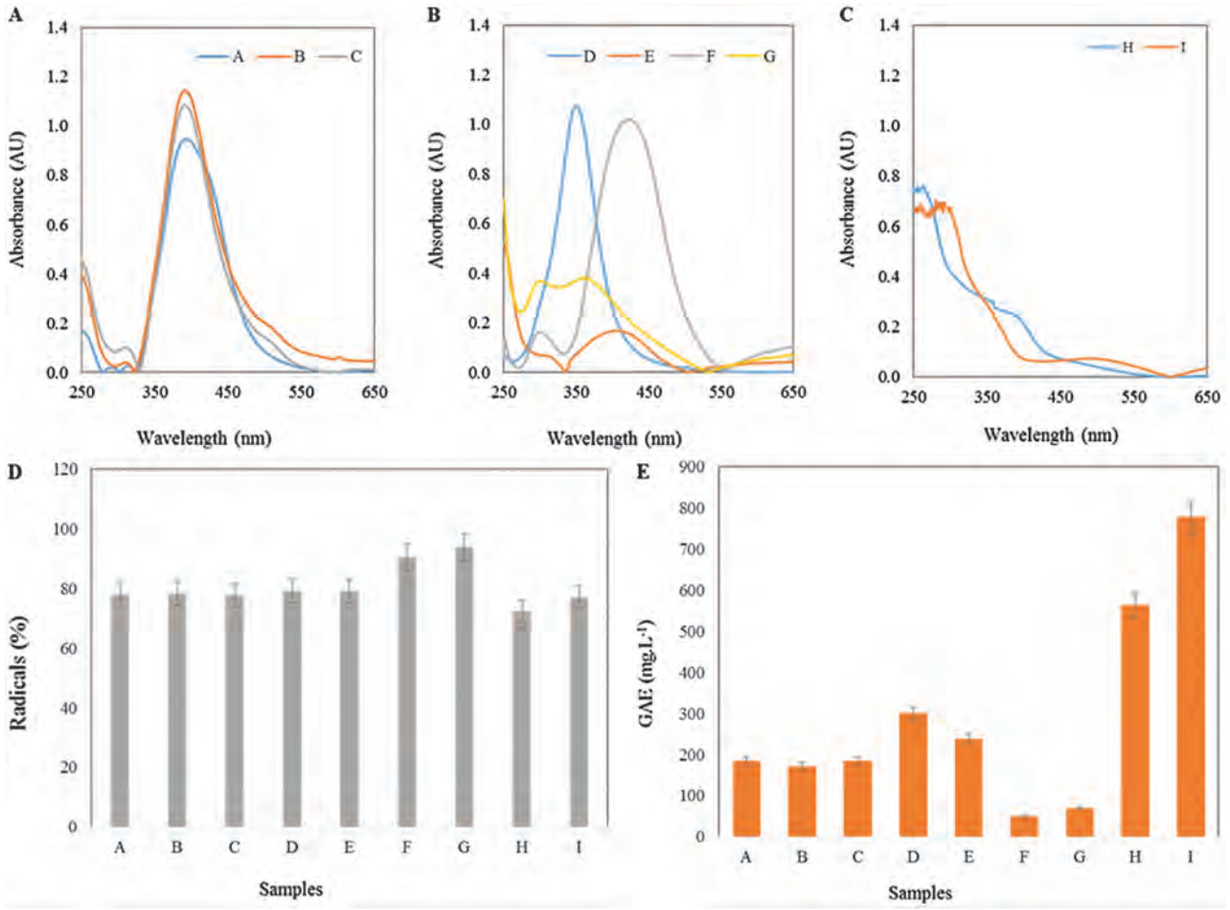

Figure 4. (A–C) UV-vis absorbance spectra of prepared AgNPs over the range from 250 to 650 nm. The concentration of analysed nanoparticles was 2 mg/mL. (D) Graph of DMPD radicals quenched by AgNPs (2 mg/mL) expressed as the percentage of remaining radicals. (E) Graph of antioxidant activity of AgNPs (2 mg/mL) measured by FR method. Further details are described in the materials and methods section.

radicals. In contrary to chemically synthesized AgNPs, the formed nanoparticles from coffee and tea extracts show the highest quenching effects (70, 73%). These results were confirmed by Free Radicals method (Fig. 4(E)) based on reducing substrate by antioxidants accompanied by a colour reaction. The results obtained clearly show that the antioxidant potential of green synthesized AgNPs (samples H and I) compared to chemically synthesized AgNPs is higher. Although, these methods for determination of antioxidant activity slightly correlate, the samples F and G show opposite trend that could be explained by different reaction mechanism of both methods.

3.4. Antimicrobial Activity of AgNPs

Agar diffusion test have been used for testing antimicrobial activity of the AgNPs examined. The method evaluates the inhibitory zones which depends on how effective the AgNPs is at stopping the growth of the bacterium. A stronger antimicrobial effect will create a larger zone, because a lower concentration of the AgNPs is enough to stop bacterial growth. Determination of the inhibition zones' sizes for *S. aureus* showed evident inhibitory effect resulting from the application of AgNPs-G and AgNPs-H with 10 mm inhibition zones. The samples A, B, F, I created on Petri dishes with *S. aureus* inhibition zones which had a size over a range from 1 to 4 mm. Figure 5(A) illustrates the lack of inhibition effect to *S. aureus* for sections C, D and E. Figure 5(B) shows antibacterial testing properties of the same samples on bacterial strain *E. coli*. Inhibition zones were created for samples B, C, G, H, I with sizes 2, 1, 3, 3, and 3 mm, respectively. Samples AgNPs-D and AgNPs-E did not cause inhibition in either of the both bacterial strains. The summary of obtained results is shown in Figure 5(C). The highest inhibition effect was shown in samples AgNPs-G, H, I for both bacterial strains.

Results obtained from measurement of inhibition zones were supported by results from growth curve method after AgNPs A–I samples treatment. The highest inhibition effects were showed by AgNPs H, I which were created by green synthesis (Figs. 6(A, B(h, i))). The concentrations 0.065, 0.52 and 2.1 mM causes totally inhibition of both bacterial strains. The minimal inhibition

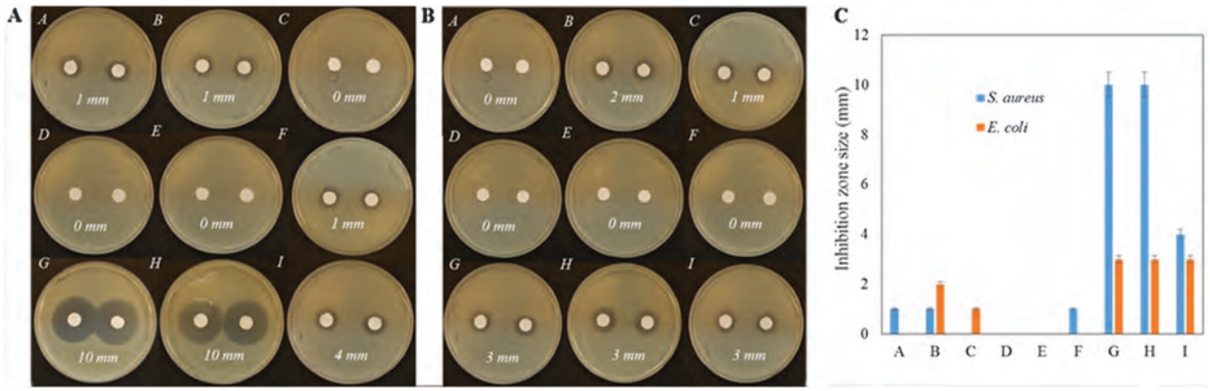

Figure 5. Comparison of inhibition zones after application of circular discs on the Petri dish with (A) *E. coli* and (B) *S. aureus* with AgNPs-A, B, C, D, E, F, G, H, I. (C) Graph of inhibition zones' sizes and the comparison between antimicrobial properties of AgNPs on *E. coli* and *S. aureus*.

concentration (MIC) was determined to be 65 μM for AgNPs in H and I samples. High inhibition effect is caused by higher concentration of $AgNO_3$ entering into green synthesis than concentration of $AgNO_3$ entering into inorganic synthesis. AgNPs samples illustrated from A–I used the same concentration of AgNPs entering into inorganic synthesis. In the *S. aureus* case, the concentration of $AgNO_3$ entering into inorganic synthesis for samples AgNPs A, B, D, F, G (Figs. 6A(a, b, d, f, g)) was determined to be 1.25 μM for the MIC. The MIC results were in this case very low which is suitable for the use of nanoparticles, signalizing the degree of bacterial resistance to antibacterial compound. The MIC values for *E. coli* were different than for *S. aureus*. The low values of MIC concentration 1.25 μM in *E. coli* case were associated with the samples AgNPs B, D, E, F. The sample AgNPs G causes totally inhibition both of *S. aureus* and *E. coli* at 160 μM concentration (Fig. 6(A), (B)–(g)).

The differences of AgNPs samples with antibacterial properties between the bacterial strains are caused by the cell wall diversity of gram-positive *S. aureus* and gram-negative *E. coli*. Gram-negative *E. coli* exhibits higher resistance than gram-positive *S. aureus*. A higher inhibition effect of AgNPs to *S. aureus* is important due to its presence in skin surface and in infected wounds. *S. aureus* is a bacteria that could be present in skin wounds. It can be easily found in hospitals where the growth of these particular bacteria in infectious diseases

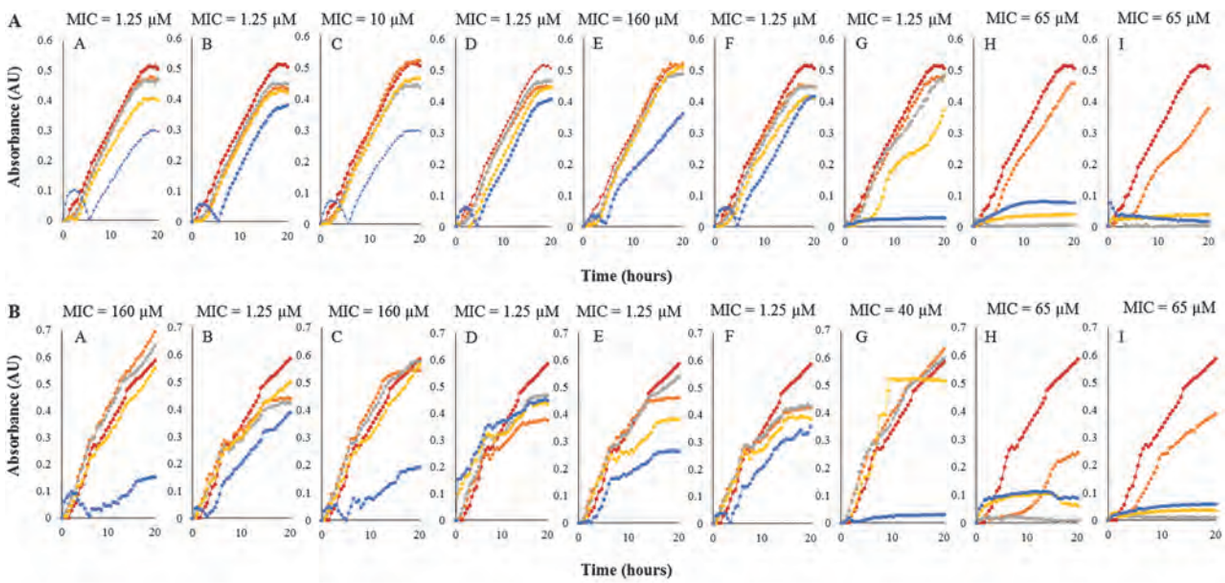

Figure 6. The growth curves of bacterial cultures with samples of AgNPs A–I is showed in A(A–I) for *S. aureus* and in B(A–I) for *E. coli*. The applications of AgNPs to bacteria was used in increasing concentrations of $AgNO_3$ entering into synthesis. The graphs show inhibition effect of AgNPs samples A–G in different concentrations (A, B(A–G)): • *S. aureus* (A), *E. coli* (B), • 1,25 μM, • 10 μM, • 40 μM and • 160 μM of $AgNO_3$. The graphs on A, B(H, I) show inhibition effect of AgNPs H and I in concentrations: • Control *S. aureus* (A), control *E. coli* (B), • 0,065 mM, • 0,52 mM, • 2,1 mM and • 8,3 mM of $AgNO_3$.

can cause severe complications to the patients. Frequently, the use of antibiotics in hospitals leads to bacterial changes such as the emergence of secondary antibiotic resistance. The most widespread resistant bacteria is methicillin-resistant *S. aureus* (MRSA). MRSA is the most common cause of incurable infections in hospital departments. Silver nanoparticles can be used as an appropriate antibacterial tool to prevent bacterial resistance forming.

Several studies indicate the dependence of AgNPs size and the antibacterial effect on ubiquitous pathogenic organisms.[2, 4, 14] The strongest antibacterial effect was found to be in small nanoparticles over the range from 1 to 10 nm^2. However, smaller AgNPs have been estimated to be toxic for tissue cells. Our synthesized nanoparticles show size *circa* 80 nm, and in the case of green synthesis they have the higher antibacterial effect than chemically synthesized AgNPs by various ways.[21]

4. CONCLUSION

In this manuscript, we have investigated the synthesis and different properties of silver nanoparticles such as their antioxidant capacity and potential of antibacterial effects. AgNPs were synthesized chemically using different reduction agents such as $NaBH_4$ and gallic acid at various pHs (8–11). Moreover, the green synthesis of AgNPs via coffee and tea extracts was also investigated. Those aforementioned synthetic (chemically and green) routes for AgNPs were investigated and compared. From our results we can observe that there is an obvious difference regarding spectral properties of AgNPs which is dependent with the way of synthesis. The green synthesized nanoparticles route gave the highest antioxidant activity as well as a significantly positive antimicrobial effect compared to the chemical synthetic route.

Acknowledgments: This project was funded from grants Anti-Microbial Coating Innovations to prevent infectious diseases (AMICI) CA COST Action CA15114. Zeta potential and particle size measurements were carried out in the Laboratory of Elemental Analysis and Structural Research, Faculty of Pharmacy with Division of Laboratory Diagnostics, Wroclaw Medical University.

References and Notes

1. P. Li, J. Li, C. Z. Wu, and Q. S. Wu, *Nanotechnol.* 16, 1912 (**2005**).
2. A. Panacek, L. Kvitek, R. Prucek, M. Kolar, R. Vecerova, N. Pizurova, V. K. Sharma, T. Nevecna, and R. Zboril, *J. Phys. Chem. B* 110, 16248 (**2006**).
3. K. B. Holt and A. J. Bard, *Biochem.* 44, 13214 (**2005**).
4. S. Shrivastava, T. Bera, A. Roy, G. Singh, P. Ramachandrarao, and D. Dash, *Nanotechnol.* 18, 225103 (**2007**).
5. S. Pal, Y. K. Tak, and J. M. Song, *Appl. Environ. Microbiol.* 73, 1712 (**2007**).
6. D. Chudobova, K. Cihalova, S. Skalickova, J. Zitka, M. A. M. Rodrigo, V. Milosavljevic, D. Hynek, P. Kopel, R. Vesely, V. Adam, and R. Kizek, *Electrophoresis* 36, 457 (**2015**).
7. M. Marini, S. De Niederhausern, R. Iseppi, M. Bondi, C. Sabia, M. Toselli, and F. Pilati, *Biomacromolecules* 8, 1246 (**2007**).
8. J. B. Ricco and O. Assadian, *Seminars Vasc. Surg.* 24, 234 (**2011**).
9. J. R. Morones, J. L. Elechiguerra, A. Camacho, K. Holt, J. B. Kouri, J. T. Ramirez, and M. J. Yacaman, *Nanotechnol.* 16, 2346 (**2005**).
10. G. A. Martinez-Castanon, N. Nino-Martinez, F. Martinez-Gutierrez, J. R. Martinez-Mendoza, and F. Ruiz, *J. Nanopart. Res.* 10, 1343 (**2008**).
11. S. Iravani, *Green Chem.* 13, 2638 (**2011**).
12. A. K. Mittal, Y. Chisti, and U. C. Banerjee, *Biotechnol. Adv.* 31, 346 (**2013**).
13. M. Ovais, A. T. Khalil, A. Raza, M. A. Khan, I. Ahmad, N. Ul Islam, M. Saravanan, M. F. Ubaid, M. Ali, and Z. K. Shinwari, *Nanomedicine* 11, 3157 (**2016**).
14. Q. L. Feng, J. Wu, G. Q. Chen, F. Z. Cui, T. N. Kim, and J. O. Kim, *J. Biomed. Mater. Res.* 52, 662 (**2000**).
15. G. Q. Wan, L. G. Ruan, Y. Yin, T. Yang, M. Ge, and X. D. Cheng, *Int. J. Nanomedicine* 11, 3789 (**2016**).
16. V. Fogliano, V. Verde, G. Randazzo, and A. Ritieni, *J. Agric. Food Chem.* 47, 1035 (**1999**).
17. M. Pohanka, J. Sochor, B. Ruttkay-Nedecky, N. Cernei, V. Adam, J. Hubalek, M. Stiborova, T. Eckschlager, and R. Kizek, *J. Appl. Biomed.* 10, 155 (**2012**).
18. P. Deepak, R. Sowmiya, R. Ramkumar, G. Balasubramani, D. Aiswarya, and P. Perumal, *Nanomedicine Biotechnol.* 45, 990 (**2017**).
19. K. Yu, F. Lu, Q. Li, H. Chen, B. Lu, J. Liu, Z. Li, F. Dai, D. Wu, and G. Lan, *Sci. Rep.* 7, 1 (**2017**).
20. M. N. Alam, N. J. Bristi, and M. Rafiquzzaman, *Saudi Pharm. J.* 21, 143 (**2013**).
21. C. Recordati, M. De Maglie, S. Bianchessi, S. Argentiere, C. Cella, S. Mattiello, F. Cubadda, F. Aureli, M. D'Amato, A. Raggi, C. Lenardi, P. Milani, and E. Scanziani, *Part. Fibre Toxicol.* 13, 12 (**2016**).

Received: 13 June 2017. Accepted: 30 September 2017.